

Lithostratigraphy and volcanic facies architecture of the Paraná Continental Magmatic Province in its NE edge with the Alto Paranaíba Arch, Minas Gerais State, Brazil

Lucia Castanheira de Moraes¹ , Hildor José Seer^{1*} , Valdecir de Assis Janasi² ,
Francisco de Castro Valente Neto¹ 

Abstract

In the NE edge of the Paraná Continental Magmatic Province (PCMP), compound pahoehoe, simple pahoehoe, rubbly flows, pillow lava, and simple pahoehoe/pyroclastic flows linked to ring structures with lithofacies associations have been identified. They belong to the Cretaceous Serra Geral Group. Intercalations of Cretaceous sedimentary deposits linked to the Botucatu Formation are common and can be of aeolian, alluvial, or, more rarely, lacustrine nature. These recurring intercalations indicate that volcanism and sedimentation occurred simultaneously and also attest to their intermittent nature. Geological characteristics of the study area — broadly dominant entablature structure, hypocrySTALLINE basalts with quench textures, types of associated sedimentary deposits, and pillow lavas — support the idea that water was present during volcanic events, especially in the central portion. The recurrence of facies associations in the same stratigraphic section is discussed and is quite different from the stratigraphy that has been described for the south of the PCMP. A preliminary investigation using P_2O_5 content allowed the identification of five P_2O_5 basalt types. The distribution of these classes in the logs shows that elaborating a valid chemostratigraphic column for the region is not yet possible.

KEYWORDS: Large Igneous Province; Paraná Continental Magmatic Province; lithostratigraphy; volcanic facies architecture.

INTRODUCTION

Large Igneous Provinces (LIPs) are found in oceanic and continental areas and include both mafic and silicic volcanic and associated intrusive rocks. Continental Magmatic Provinces (CMPs), which are the best-described type of LIP, have been studied worldwide since the last decades of the 19th century. Several factors are responsible for the interest in CMPs, especially their role in climate change and mass extinction, and the fact that they represent Earth's largest short-lived igneous events. In addition, they are useful in paleocontinental reconstruction, providing temporal frames for stratigraphic correlation, and allowing the test of models of magma generation (Bryan and Ernst 2008, Jay and Widdowson 2008, Jerram and Widdowson 2005, Wignall 2001, 2005, Self *et al.* 2006, Chenet *et al.* 2009).

The Paraná Continental Magmatic Province (PCMP) has also been studied since the end of the 19th century. Despite the advance in the understanding of its geological history, several points remain obscure. Importantly, the current knowledge level along its vast extension is uneven, with the northern portions in Brazil, notably in the Minas Gerais area, being much less studied in comparison with the southern part of the province.

Recent research on the Serra Geral volcanism in SW Minas Gerais (Moraes and Seer 2018, Moraes *et al.* 2018) presented new data on the facies architecture, petrography, and petrology of basalts in this region. In this paper, the study area was enlarged, and the flow morphologies were detailed, allowing us to advance also in the understanding of the emplacement of volcanic rocks and environmental conditions.

GEOLOGICAL CONTEXT

The study area is located in the Minas Gerais State, Southeastern Brazil, within a polygon bounded by the extreme coordinates 47°32'21" W/49°16'27" S and 18°23'27" S/18°58'49" S (Figs. 1 and 2). The basement consists of schist, quartzite, and gneiss, comprising the Araxá Group, part of the Brasília Neoproterozoic Orogen that borders the São Francisco Craton. Over these rocks, aeolian to alluvial sediments of the Botucatu Formation — formed in a Lower Cretaceous desert — were deposited. The Serra Geral flood basalt volcanism, with intercalations of aeolian, alluvial, and lacustrine sediments, is, in part, contemporaneous with

Supplementary data

Supplementary data associated with this article can be found in the online version: [Supplementary Table](#).

¹Centro Federal de Educação Tecnológica de Minas Gerais – Araxá (MG), Brazil. E-mails: 2013luciam@gmail.com, hildorseer@cefetmg.br, fcvn.araxa@cefetmg.br

²Universidade de São Paulo – São Paulo (SP), Brazil. E-mail: vajanasi@usp.br

*Corresponding author.



the Botucatu Formation. During the Upper Cretaceous, the region received sedimentation of conglomerates and sandstones of the Bauru Group that locally cover this sequence. In the extreme east, the maximum thickness of the Botucatu Formation added to the Serra Geral Group is 100 m — which is confirmed in the Sacramento region (Moraes *et al.* 2018) —,

while in the west end of Canápolis, the minimum thickness of Serra Geral Group is 200 m, and the Botucatu Formation does not outcrop. In general, the contacts between these two units and between lithological units of the Serra Geral Group can be traced in agreement with the elevation, which is not always true for the contact between them and the Late Proterozoic basement.

The filling of basement paleovalleys began with aeolian or alluvial fan sedimentation even if, in some places, this filling was only completed with basalt flows. They dominantly represent compound pahoehoe, simple pahoehoe, and rubbly flows, which can be recurrent in the stratigraphic record. Intertrap sedimentation is frequent, although not expressive in volume, and the deposits may be aeolian, alluvial fan, or, more rarely, lacustrine. These recurring intercalations indicate that both processes — volcanism and sedimentation — occurred simultaneously and also attest to their intermittent nature. Occasionally, the contact between sedimentary and basaltic rocks shows interaction forming peperites/pseudopeperites, grooves produced by basalt flows on the still unconsolidated surface, and degassing pipes in sandstone, as well as infiltration of sediments in the brecciated top of basalt flow.

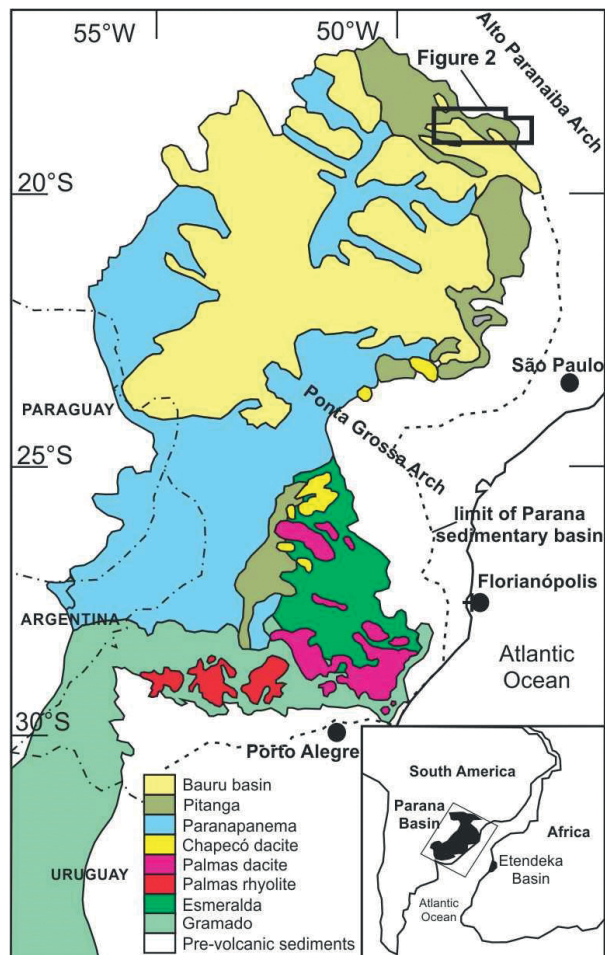


Figure 1. Geological sketch of the Paraná Continental Magmatic Province with its magmatic rocks distribution overlapped by the Bauru Basin and location of the research area (Fig. 2). Modified from Janasi *et al.* (2011) and Waichel (2006).

METHODOLOGY

Seventy-seven outcrops (FIT01 to FIT77), which occur especially in road sections, quarries, and river beds, were visited and described. Even if the exposures are not continuous and the outcrops are often weathered and/or covered by colluvium, eight detailed logs were built from the basement to the Upper Cretaceous rocks that cover the Serra Geral Group; additional more punctual logs were also built. Field data together with the data presented by Moraes *et al.* (2018) and the SRTM Digital Terrain Model, corrected by the National Institute for Space Research (*Instituto Nacional de Pesquisas Espaciais* — INPE) (Valeriano 2004), allowed the construction of the geological map (Fig. 2) in a QGIS software environment. Also, the lava structures and morphology identified allowed us to advance in understanding

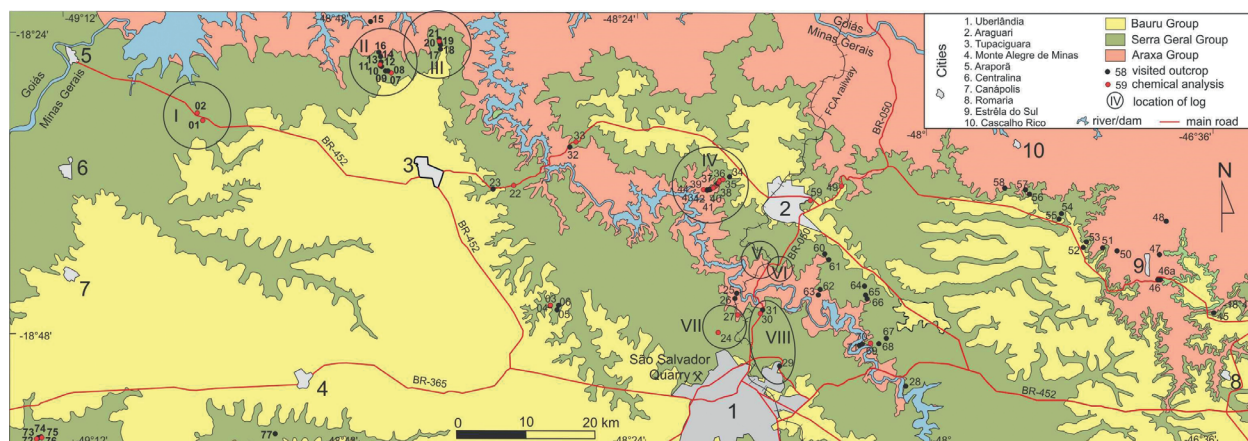


Figure 2. Geological map of the research area with logs and location of the studied outcrops and cities. Outcrops were represented without their first name (FIT). Note that at this scale, the Botucatu Formation cannot be represented. Compiled from the mapped areas in the Triângulo Mineiro Project (Pedrosa-Soares *et al.* 2017).

the volcanic processes that occurred in the region, even if no quantification has been attempted.

Besides primary characteristics of lava flow, such as lithology, structures, and texture patterns, the results presented were based on petrographic studies of 46 samples. Petrographic studies were performed on 28 thin sections at the Universidade de São Paulo petrographic laboratory.

Field criteria used by Rossetti *et al.* (2014) and Barreto *et al.* (2014) — facies analysis method, based on McPhie *et al.* (1993), Miall (1996), Walker (1984), Jerram (2002), among others — were employed in the data analysis presented herein. Red points in Figure 2 show outcrops where 22 whole-rock geochemistry analyses (oxides and trace elements) were carried out (for geochemistry data table, see the online version of this article) (Supplementary Table).

LITHOFACIES ASSOCIATIONS IDENTIFIED IN THE RESEARCH AREA

The lithologies, structures, and textures identified were associated according to their form of occurrence and grouped into lithofacies. Facies and lithofacies association methodology, together with lithochemochemistry, has been increasingly used and allowed considerable advances in the understanding of CMPs (for example, Single and Jerram 2004, Waichel *et al.* 2012, Duraiswami *et al.* 2014, Barreto *et al.* 2014). In this sense, Table 1 presents the descriptive characteristics that define lithofacies, a code for their easy and quick identification, and the interpretation of their positions in the volcanic succession.

These lithofacies were grouped in associations, which comprise compound pahoehoe, simple pahoehoe, rubbly flows, simple pahoehoe/pyroclastics, and pillow lava (Tab. 2). The last two lithofacies associations are limited in area, while the first three are widely distributed and may be recurrent in the stratigraphic column (Fig. 3). In general, basalt flows cover sediments of the Botucatu Formation, but in at least three places, they rest directly on metamorphic basement rocks. The pillow lava lithofacies association, already discussed in Moraes and Seer (2018), is also cited in Table 2.

Compound pahoehoe lithofacies association

Compound pahoehoe lithofacies association is characterized by lobes with thickness ranging from 0.2 m to 2 m, stacked vertically and laterally (Tab. 2; Figs. 4A, 4B, 4C, and 4D). Generally, the external lobe surface is smooth, and its margin is chilled and oxidized, but its interior shows millimeter to centimeter-sized vesicles well distributed in a hypocrySTALLINE rock (Figs. 4E and 4F). Vesicles, which are filled with silica, celadonite, and, eventually, zeolites, may reach 4 cm in diameter. These attributes characterize S-type lobes (spongy; Walker 1989). Flow overlapping can reach thicknesses up to 17 m. Some lobes are massive, even if most of them are irregularly fractured. According to Self *et al.* (1998), “*P-type flows typically have a dense interior and more vesicular exteriors, the exact opposite of S-type lobes. S-type lobes form with minimal*

inflation, whereas inflated lobes invariably have the basic characteristics of P-type lobes.”

These rocks are hypocrySTALLINE, rich in plagioclase, clinopyroxene, and opaque minerals besides olivine. Microphenocrysts (up to 1 mm) are rare, while microliths (up to 0.2 mm) are abundant and immersed in a glassy matrix. Plagioclase occurs as thin laths with swallow-tail termination, and pyroxene is subeuhedral and fractured, whilst olivine crystals are euhedral, usually transformed into iddingsite, and a few have well-preserved nuclei (Figs. 4H, 4I, and 4J). This association is present at the top of Log 1 and the base and top of Log 2 (Fig. 3).

Simple pahoehoe lithofacies association

This association is distinguished by the tabular geometry of individual basalt flows, with greater than metric lateral extension (the poor quality of the outcrops makes determining the size difficult), thickness between 0.6 and 7 m, and an internal structure of basal zone, massive core, and an upper vesicular

Table 1. Lithofacies summary description, code, and interpretation for basaltic rocks from Ituiutaba — Estrela do Sul region, NE edge of the Paraná Continental Magmatic Province.

Description	Code	Interpretation
Aphanitic vesicular basalt	Bav	S-type lobe
Aphanitic basalt with vesicular layer	Bavl	Basalt lobes with gas segregation structures
Aphanitic basalt with vesicle cylinder	Bavc	Basalt lobes with gas segregation structures
Aphanitic massive basalt	Bam	Lava flow core
Basalt with prismatic or irregular joint	Bpj	Lava flow core with entablature
Basalt with regular prismatic joint	Brpj	Lava flow core with colonnade
Vesicular basalt with horizontal joint	Bvhj	Lava flow base or top
Basalt with vesicle cylinder or proto-cylinder	Bvc	Lava flow core
Vesicular basalt up to one centimeter	Bv	Upper half of the lava flow core – viscoelastic zone
Vesicular basalt with geodes	Bvg	Upper half of the lava flow core – viscoelastic zone
Flow-top vesicular breccia	Bvb	Lava flow brecciated upper crust
Pillow basalt with hyaloclastite	Bpw	Pillow lavas mixed with sediments and hyaloclastites
Peperite/pseudopeperite	Pp	Interaction between lava and unconsolidated sediments
Aeolian sediments	Sa	Formed in an arid and windy environment
Alluvial fan sediments	Saf	Formed by rapid and intermittent aqueous flows
Lacustrine sediments	Sl	Formed in a dam water environment

Table 2. Facies association and flow morphology/Lithofacies associations of the study area.

Sketch	Facies Association	Description	Interpretation
	Compound Pahoehoe	S-type lobes with thickness up to 2 m, stacked in a heterogeneous braided pattern and showing a holocrystalline and vesicular or massive core with thin glassy surface, generally oxidized	Low effusion rate with intermittent lava supply
	Simple Pahoehoe	Tabular lobes with thickness ranging from 0.6 to 15 m and internal structure consisting of massive core and upper vesicular zone. Generally, the contact between adjacent sheets is marked by a thin glassy edge, but a thin layer of red bole may be present. Segregation structure-like	Low effusion rate with sustained lava supply. Lava solidified under a semi-solid carapace, with minimum inflation
	Rubbly flow	Thick lava flows (> 8 m) showing tabular geometry with a <i>not always visible</i> centimetric vesicular base, a holocrystalline core (Bam) with irregular columnar joint (Bapj) and vesicle-rich upper portion (Bv), in addition to flow-top vesicular breccias (Bvb).	Effusion rate higher than the previous ones with sustained lava supply and autobrecciation of flow upper crust
	Simple Pahoehoe/pyroclastics	Tabular lobes with thickness < 3 m, sharp top and base contacts, and, sometimes, showing gentle dips (up to 7°) toward the external part of the ring structure. Internal structures comprise irregular columnar joint in the core and a top rich in vesicles up to 0.3 cm. The flows are covered by tuffs, lapilli, scoria, and variations between them, already well-weathered Bapj, Bv, and Bam can be present	Basaltic and pyroclastic ring structure probably formed when the temperature was cool enough to crystallize almost all the fissure surface, leaving some circular spots as lava lakes. Pyroclastic material was probably produced by phreatomagmatic-associated processes
	Pillow lava and lacustrine sediments	Packages of pillows – separated by pahoehoe lobes – vary from densely packed to dispersed in the middle of intensely deformed sediments, which consist of fine sandstones, clayey sandstones, sandy argillites, and argillites, in addition to hyaloclastites.	In a peridesertic environment with intense but irregular rains, a lake may have been formed by the irregularity of the paleorelief or by a barrier generated by volcanic flows. When the basalt flow reached the top of the barrier, it could enter the lake, plunging into the deposited sediments. The massive basalt between the sets of pillow lava is tentatively explained by the intermittence of the lake.

zone. Flow overlapping, which cannot always be individualized, can reach thickness up to 12 m. The boundary between the basalt flows generally gives rise to a region of weakness and water percolation. This secondary process facilitates their identification in the field, as does an oxidized surface. In thicker flows, colonnades (which vary between 0.6 to 1.3 m in diameter) develop at the base and/or the top, while entablature occurs at the central portion (Fig. 5A). Nevertheless, entablature (up to 0.3-m thick) and/or irregular fracturing largely predominate (Fig. 5C). The upper vesicular zone is up to 100-cm thick. The basalt in this zone is hypocrySTALLINE, and vesiculation is gradational, with vesicles becoming smaller and less abundant upwards; the process is usually recurrent (Fig. 5E). Vesicle cylinder associated with geode is a common feature

in the FIT24 quarry (Fig. 5D). Other examples of segregation structures can be seen at this quarry; however, they are not as common as described in other occurrences in the Province (e.g., Barreto *et al.* 2014). In addition to the vesicular viscoelastic surface, the top of the sheet flows can be marked by the presence of tumulus and, locally, by bole rich in rubble, in the sense of Single and Jerram (2004) (Figs. 5A and 5B).

In general, the core is holocrystalline, fine-grained, with plagioclase and pyroxene as microphenocrysts (both up to 3 mm) surrounded by a matrix rich in prismatic microlite of granular pyroxene, and/or needle plagioclase and opaque mineral in skeletal and needle form. Apatite occurs clustered in plagioclase crystals. The intergranular texture is dominant, although the presence of interstitial murky brown glass and diktytaxitic



Figure 4. Compound pahoehoe lithofacies association: (A) FIT22; (B) FIT02; (C) FIT22; (D) FIT77: different aspects of compound pahoehoe lobes; (E) FIT1A: S-type lobe, yellow arrow shows chilled margin; (F) FIT77: More oxidized S-type lobe with bigger vesicles than in E; (G) Contact between two lobes with weathered glass from upper and basal crusts of both in FIT22; (H) General aspect of the FIT22 thin section: rare microphenocrysts and abundance of plagioclase crystals and glass; (I) zoom of the same FIT22 showing the skeletal appearance of plagioclase, already altered olivine crystals — lower central portion —, and the vitreous matrix (vm); (J) In the FIT12 thin section, besides the vitreous matrix and altered olivine crystals, the granular aspect of pyroxene crystals and swallow-tail termination of plagioclase are clear.

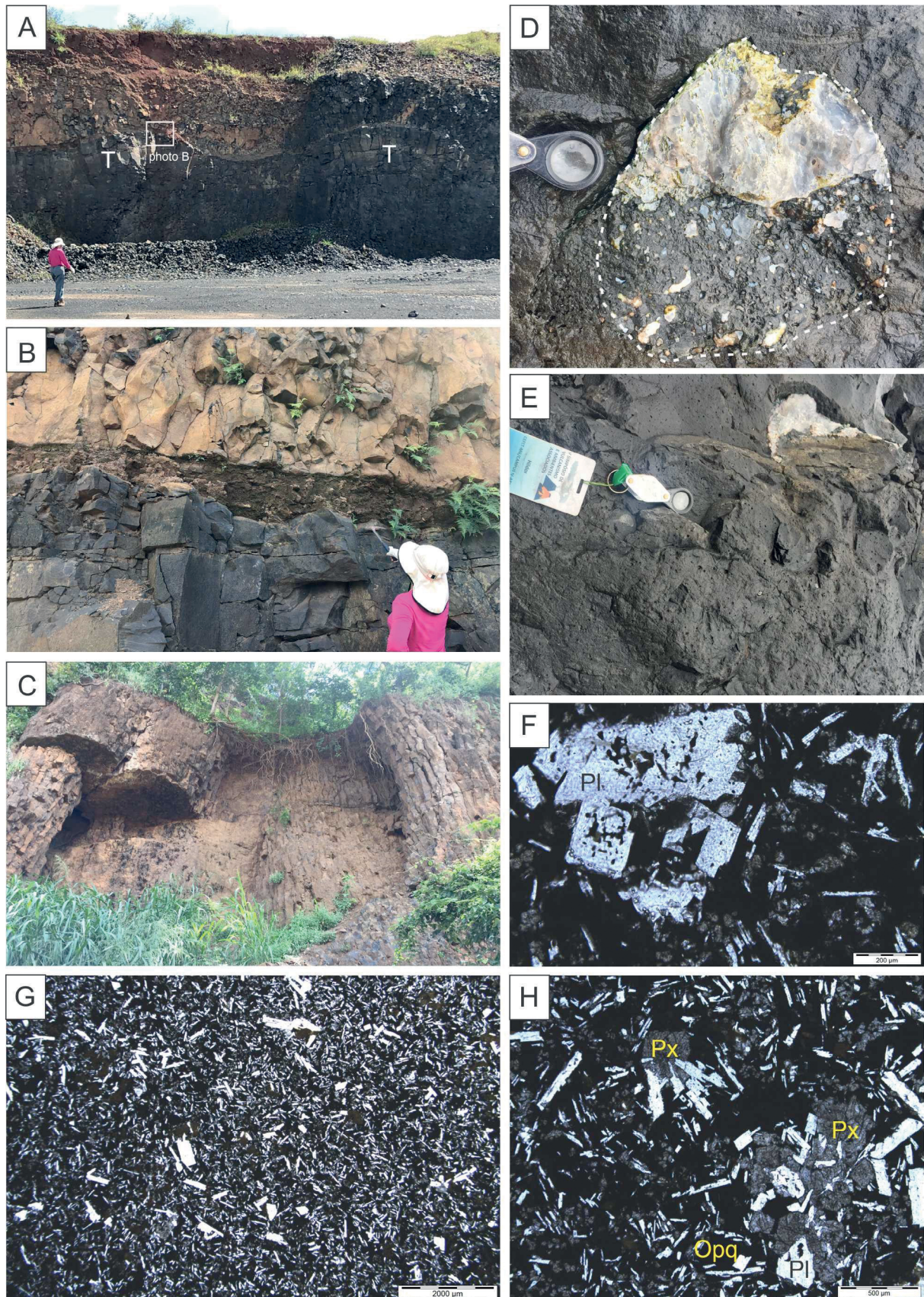


Figure 5. Simple Pahoeohoe Lithofacies Association: (A) general view of FIT24, with irregular fracturing near the base of the quarry and colonnade pointing out the flow-top, where a well-developed tumulus structure (T) can be seen. It is covered by a red bole (detail in B). The flow above the red bole is rubbly; (B) the red bole is essentially a weathered material and is not disturbed by the flow above it; (C) expressive entablature in the flow core (FIT07), which, associated with master joints, generated large, rounded, about 10-m tall columns; (D) vertical view of the FIT24 viscoelastic portion rich in vesicles and showing a mushroom-shaped geode; (E) top view of a vesicle cylinder inside a FIT24 viscoelastic portion; (F) photomicrograph showing plagioclase microphenocrysts rich in fluid inclusions immersed in a mesostasis with microliths of plagioclase, pyroxene, opaque mineral, and abundant glass (FIT24); (G) general aspect of the thin section where intergranular texture and two generations of plagioclase and opaque minerals are clear (FIT24); (H) subophitic texture and abundant glass in a devitrification process. F, G, and H are under parallel polarizers.

texture are conspicuous in the viscoelastic region. This facies has the greatest abundance of phenocrysts in the study area (Figs. 5F and 5G). The presence of fluid inclusions in plagioclase microphenocrysts is noteworthy (Fig. 5F). Subophitic and glomeroporphyritic textures are not rare (Fig. 5H).

We underline that two of the described outcrops depart somewhat from the 'sheet flow' pattern (for example, FIT07); they are thicker than average (up to 15 m), homogeneous, have entablature, and appear to be uniformly aphanitic, but segregation structures were not seen. Neither base nor top was observed, making interpretation difficult. FIT07 also shows regular and near-vertical master joints, which generate unusually rounded and homogeneous columns when broken (Fig. 5C). They are analyzed in the Discussion section.

Rubbly flow lithofacies association

Rubbly basalt flows are common and outcrop in several logs, as shown in Figure 3 (Logs I, II, IV, VI, and VII) and the São Salvador quarry (Fig. 2, SW of Profile VII). Typical morphology shows an incipient vesicular basal crust, a massive core, and a brecciated and scoriaceous upper crust, which can constitute up to 1/3 of the total flow. These are the thickest flows seen in the study area. Where exposed, rubbly flows cover alluvial deposits, simple pahoehoe lithofacies, or other rubbly flows and are recovered by compound pahoehoe, simple pahoehoe, rubbly lithofacies association, or sedimentary rocks of the Bauru Group.

Basal crust shows black aphanitic basalt with millimeter-sized vesicles. Characteristically, the core comprises about 2/3 of the flow and is intensely fractured in an irregular pattern (Fig. 6A) or a splintery curved columnar pattern (Fig. 6B). Colonnade occurs locally. Basalt can be black or reddish-brown, indicating oxidation. Locally, an exotic radial columnar jointing pattern with brecciated material in the center is observed; this pattern was described by Moraes *et al.* (2018) as rosettes. Toward the top, a viscoelastic portion is found, formed by aphanitic basalt with a profusion of amygdaloids filled with chalcedony and/or celadonite (up to 3 cm, Figs. 6A and 6D); locally, geodes are filled with chalcedony, quartz, or amethyst, besides gas blister. Not rarely, the viscoelastic portion shows intense fracturing filled with zeolites and chalcedony (Fig. 6D). The brecciated top crust is dominated by fragments of vesicle-rich hypocrySTALLINE basalt. The dimensions of the fragments vary from millimeter to decimeter and from angular to sub-rounded (Figs. 6C and 6E); the fragments may be cemented by zeolites, silica, or hypohyaline to hypocrySTALLINE basalt. Locally, voids between fragments may be filled with sediments.

The basal crust and viscoelastic portion are aphanitic and hypocrySTALLINE, with crystals (< 0.5 mm) of plagioclase, pyroxene, opaque minerals, and occasionally olivine surrounded by abundant partially devitrified glass; vesicles are up to 1-mm large (Fig. 6F). Usually, the core is hypocrySTALLINE and aphyric, characterized by intersertal and intergranular texture domains (Fig. 6G). Crystals of plagioclase, clinopyroxene, opaque minerals, and occasionally olivine are arranged between interstitial glass; rare vesicles are smaller than 1 mm. Olivine forms the largest crystals (≤ 1 mm) and shows rare portions preserved

amid corrosion and alteration. Plagioclase laths, clinopyroxene grains, and opaque mineral tend to be euhedral, but, when associated with devitrification, the last one is needle-shaped (Fig. 6H).

Simple pahoehoe/pyroclastics

Some small ring structures were seen in this area through satellite images — one in a small river (Brejo creek) that crosses the city of Araguari and another in the Tijuco River bed, west of Monte Alegre de Minas — their location is indicated on the map (Fig. 2 — FIT59 and FIT72). At FIT59, exposure is partial, and the river receives sewage, which makes access almost impossible. Lobes that gently plunge out of it in an annular arrangement can be seen, but no volcanoclastic deposits have been found. The lobes are decimetric — 0.2 to 0.5 m —, vesicular, and irregularly fractured, with some tendency to show columns with curvilinear edges and/or triple junction.

The small ring structure showed in Figures 7A and 7B, among others, is about 10 m in diameter, two-thirds of which are exposed in the dry season, when the water level drops considerably. From the ring structure, pahoehoe lava flows of metric thickness and dipping gently (up to 7°) outward stack up sideways and vertically (Figs. 7B and 7C). They show irregular columns (up to 0.3-m wide) in aphanitic dark gray basalt with sparse microamygduloids. Microscopically, the basalt shows plagioclase, clinopyroxenes, opaque minerals, and microamygduloids (all ≤ 0.5 mm) in an intersertal and rarely subophitic texture, with interstitial plagioclase, pyroxene microlites, and dark brown glass being partly replaced by opaque mineral needles, in addition to iddingsite and celadonite (Fig. 7E).

Radial, but dominantly WNW- and NE-oriented fractures present in the pahoehoe lava flows are remarkable; most of them are apparently secondary or, at least, reactivated. Volcanic lobes are covered by volcanoclastic rocks, specially lapilli tuffs with sparse fragments of up to 0.10 m that vary from massive to strongly vesicular (Fig. 7D). Exposition is 5- to 7-m thick and occurs in a weathered and intensely vegetated area, in such a way that the preserved material is reduced to loose blocks. The pyroclastic samples studied are dominated by hypohyaline basalt lithic fragments and occasional volcanic crystal fragments, with minor accidental siliciclastic contribution. The accidental siliciclastic contribution is formed by well-rounded quartz grains with medium to fine sand size, disperse in the rock (Fig. 7F), as well as more angular grains with fine sand and silt size, which are locally abundant and mixed with clay and volcanic ash (Figs. 7F and 7G). Among the volcanic contribution, glass fragments predominate. Typically, shards show corrosion gulfs and sharp edges with greenish outer film indicating reaction. Hypohyaline basalt lithic fragments contain plagioclase microphenocrysts and amygduloids filled with silica and locally resemble pumice for the abundance of vesicles. Volcanic crystal fragments can be pulverized plagioclase, pyroxene, and opaque mineral, with broken and sharp edges.

Lapilli tuffs may show sedimentary lamination that can be locally convoluted (Fig. 7G). Where observed, the basalt flow/pyroclastic rock contact appears to be invasive and irregular, locally with pockets of pyroclastic material within the flow;

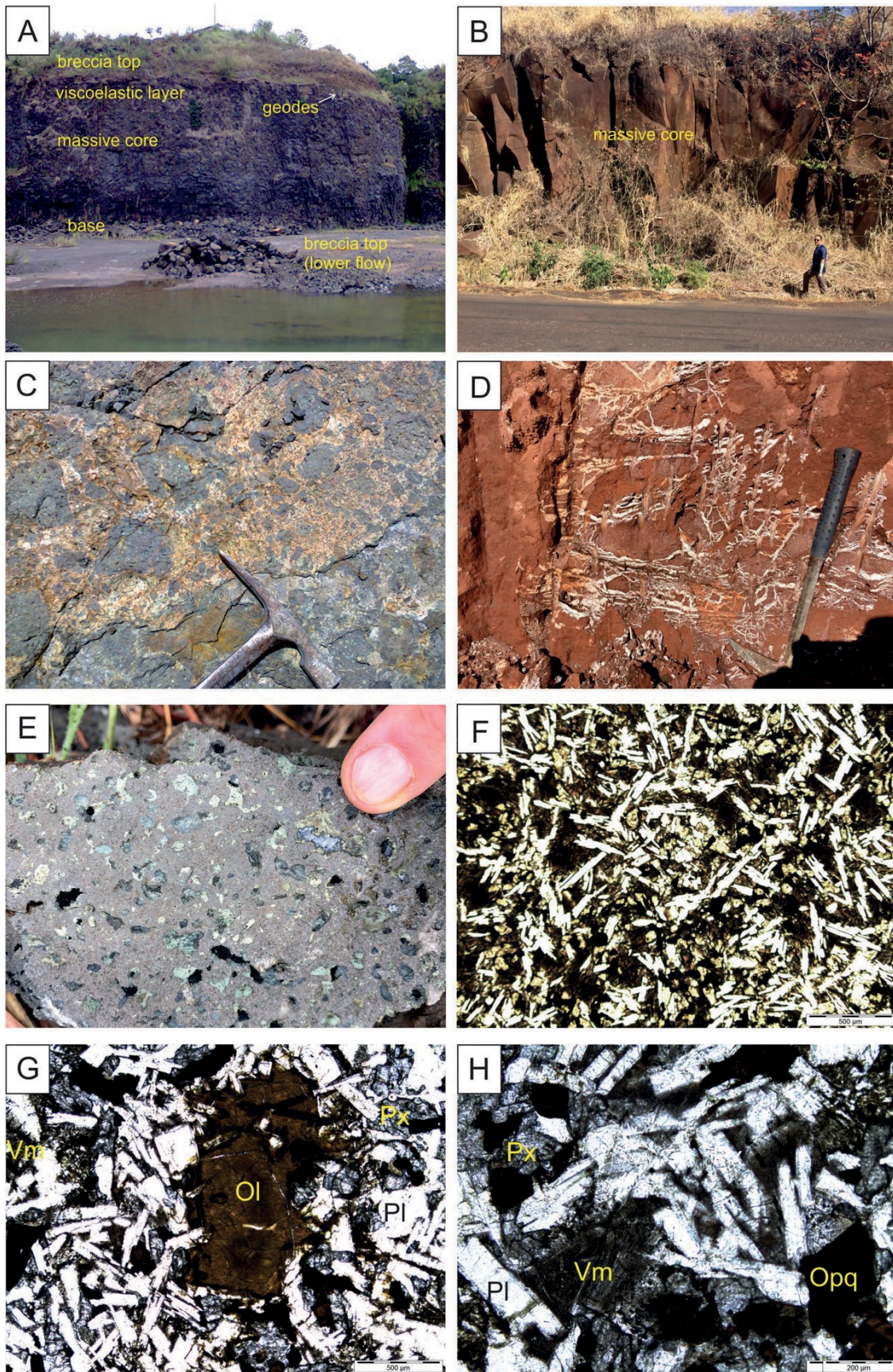


Figure 6. Rubbly Lava Lithofacies Association: (A) exposition of complete rubbly flow drawn in Table 2 — São Salvador quarry (see Fig. 2 for location); (B) splintery curved columnar pattern in the FIT02 core; (C) brecciated top crust from the basal flow in photo 6B; (D) fracturing filled with zeolites and chalcidony in viscoelastic portion — São Salvador quarry; (E) top crust fragment intensely vesiculated (FIT01); (F) viscoelastic portion in thin section; abundant plagioclase, pyroxene, and opaque microlites in an intergranular texture, with interstitial glass in devitrification process; olivine altered to iddingsite and microvesicles are present (FIT40); (G) olivine microphenocryst altered to iddingsite, plagioclase and pyroxene microlites in an intersertal texture with abundant interstitial glass in devitrification process, rich in opaque needles (FIT02); (H) two generations of opaque minerals; the last one as needles from devitrification (Vm = vitreous matrix), which lends a dirty appearance to the thin section (FIT02). Photomicrographs F, G, and H are under parallel polarizers.

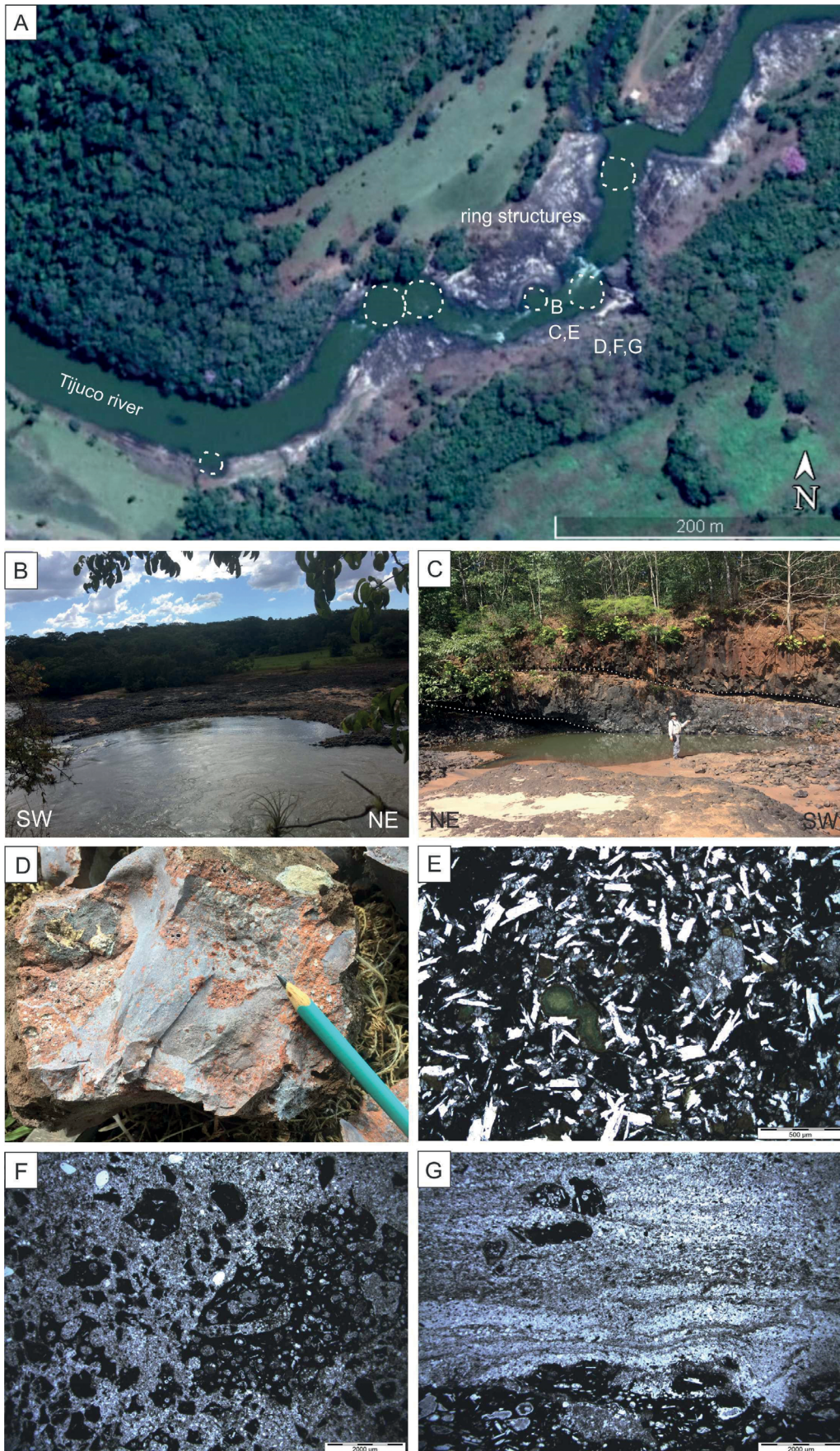


Figure 7. Simple pahoehoe flows and pyroclastic linked to ring structures: (A) Google Earth Image (07/26/2019 — CNES/Airbus, 18°56'30.4"S/49°15'35.5"W) showing at least six ring structures (possibly nine) at the Tijuco River bed and the next photo localization, all related to the B structure; (B) general view of the studied ring structure, with stacked lobes in the background; ((D) lapilli tuff with rare breccia fragments (FIT75); (E) aphyric and hypocrySTALLINE basalt, with abundant microlites, microamygdules, and interstitial glass; (F) thin section of lapilli tuff rich in basaltic and vitreous shards, sparse well-rounded grains of quartz in medium sand granulometry in a matrix rich in quartz, plagioclase, pyroxene, and ash (FIT74); (G) disturbed lamination of volcanic ash with sparse vesicle-rich shards (FIT75B). Photomicrographs E, F, and G are under parallel polarizers.

in this case, basalt is vitreous with amygdules and scattered plagioclase microlites.

ASSOCIATED SEDIMENTARY DEPOSITS

Sedimentary rocks occur as aeolian, alluvial, and lacustrine deposits. Locally, fluvial sediments seem to be associated with the last two. Aeolian deposits are essentially sandstone, while the other two are quite diversified, as shown in the logs of Figure 3.

Lacustrine deposits were described by Moraes and Seer (2018); thus, we limited the study to describing alluvial and aeolian deposits representative of the area.

Alluvial deposits range between 0.2- and 5-m thick, while the aeolian ones vary between < 1 and 40 m. Besides those described by Moraes and Seer (2018), only one limited occurrence of lacustrine deposit was found; both are concentrated around the Araguari-Uberlândia region. From there to both east and west, aeolian deposits prevail.

Typical fluvial-alluvial deposits are present across Log 4 and described in detail hereafter. Above the eroded and irregular surface of the muscovite-quartz-schist, a *first* fluvial sequence (ca. 4-m thick) is present. In it, several small channels (between 30- and 50-cm wide) alternate and intercalate with two 10-cm thick layers of medium to coarse grain-sized pink sandstone, with sparse pebbles up to 5 cm in diameter. The clast-supported conglomerate which fills the channels has pebbles (up to 6 cm in diameter; an average of 2 cm) of milky quartz and granite, and matrix consisting of quartz, muscovite, feldspar, and clay-minerals cemented by iron oxide (Figs. 8A and 8B). Under the microscope, the sandstone is coarse, with quartz, K-feldspar, muscovite, opaque minerals, quartzite, and apatite. Grains are sub-rounded to rounded and cemented by chalcedony. The sequence is covered by fine, black basalt.

An interruption in the volcanic event is registered 31 m above, with a *second sedimentary sequence* ca. 3–4-m thick. It begins with a matrix-supported conglomerate sandstone, presenting granules and small pebbles of quartz, quartzite, shale, and basalt. The presence of well-rounded quartz grain contribution is negligible, and the grains decrease in size to silt-clay. The silt-clay fraction is transformed into greenish chert, with deformed banded and vugs, whose walls are adorned by delicate quartz crystals. Under the microscope, the sandstone is medium to fine-grained, with subangular to angular grains, and rich in quartz and muscovite, with less biotite, opaque mineral, apatite, K-feldspar, and zircon.

This sequence is covered by a second 33-m thick basalt flow that, in turn, is covered by a *third*, poorly exposed, ca. 4-m thick sequence of sedimentary rocks with alluvial fan characteristics. It begins again with conglomerate sandstone, whose sub-rounded to angular fragments do not exceed 1.5 cm, succeeded toward the top by sandstone, siltite, and argillite. The siltite resembles a chert, which can be a thermal effect of contact with a third basalt flow covering it. This hypothesis is corroborated by interaction features, such as fluidization with fragmentation, formation of amygdules and gas escape

channels, and atectonic folds (Figs. 8C and 8D). In the thin section, siltite shows parallel lamination, fractures, and vugs, with the last two filled with chalcedony. It is dominated by angular to subangular quartz grains, with contribution of muscovite, opaque mineral, K-feldspar, zircon, tourmaline, and quartzite. Well-rounded grains are restricted.

After the third basalt flow, which is incompletely exposed and has an estimated thickness of 13 m, a *fourth*, ca. 5-m thick sedimentary sequence of alluvial nature occurs. It starts with a matrix-supported conglomerate with a sandy matrix, followed by an immature conglomerate sandstone with silt-clay contribution. These rocks show fractures (generating breccia) and fluidization, with elongated vugs whose walls are covered by zeolites, as well as lamination disturbance and small normal faults. As a result of the contact with the fourth basalt flow that covers the sequence, a peperite was formed.

In the thin section, sand terms tend to be lithic, rich in quartzite and phyllite fragments, but dominated by quartz with contribution of K-feldspar, plagioclase, muscovite, garnet, epidote with traces of zircon, and kyanite. Siliceous cement corrodes the grain edges. Other lithotypes identified are: immature fine sandstone (Fig. 8E) with quartz grains from very angular to very well-rounded and with volcanic glass, probably torn from the vitreous crust of the lower basalt flow. Volcanic lithoclast edges are strongly altered, and the presence of celadonite in the matrix is conspicuous. In the FIT38D sample (Fig. 8F), the well-rounded grain contribution is less important, and the grano-decreasing stratification is striking.

The 33-m thick fourth basalt flow — which disturbs the described sequence, generating peperite — is covered by a thin alluvial sequence — *the fifth* —, suggesting a new small interruption in magma supply. This sequence has two levels: the lower one — lenticular and with less than two meters — is a reddish, medium to coarse immature sandstone, with basalt fragments, while the upper level — around one-meter thick — is a massive conglomerate sandstone — with fragments up to 5 cm —, produced by a rapid sedimentary flow. The conglomerate sandstone is covered by a fifth poorly exposed basalt flow around 40-m thick. The top of this flow eroded and was later covered by sandstones of the Bauru Group.

Records of lava/sediment interaction are not uncommon in the study area. For example, FIT53 starts with an alluvial deposit lying over the basement, where channels filled with lithic pebbles and quartz sand pass gradually into sandstone with well-rounded quartz. The first one has a thickness of around 2 m, and the second reaches 46 m. At the top, it is possible to see evidence of lava flow over the unconsolidated sandstone.

Most of the dominant well-rounded sandstones were deposited directly on the basement, but some are intertrap. Most intertraps have thicknesses lower than 1 m, but some reach 5 m (FIT18, 19, 47). The thicker occurrences show large-scale, high-angle, cross-stratification, but low-angle cross-stratification can also happen (Fig. 8G). Asymmetrical wind ripples, sometimes with interference and bimodality — given by alternating lamination of medium and fine sand —, are conspicuous characteristics (Fig. 8H).

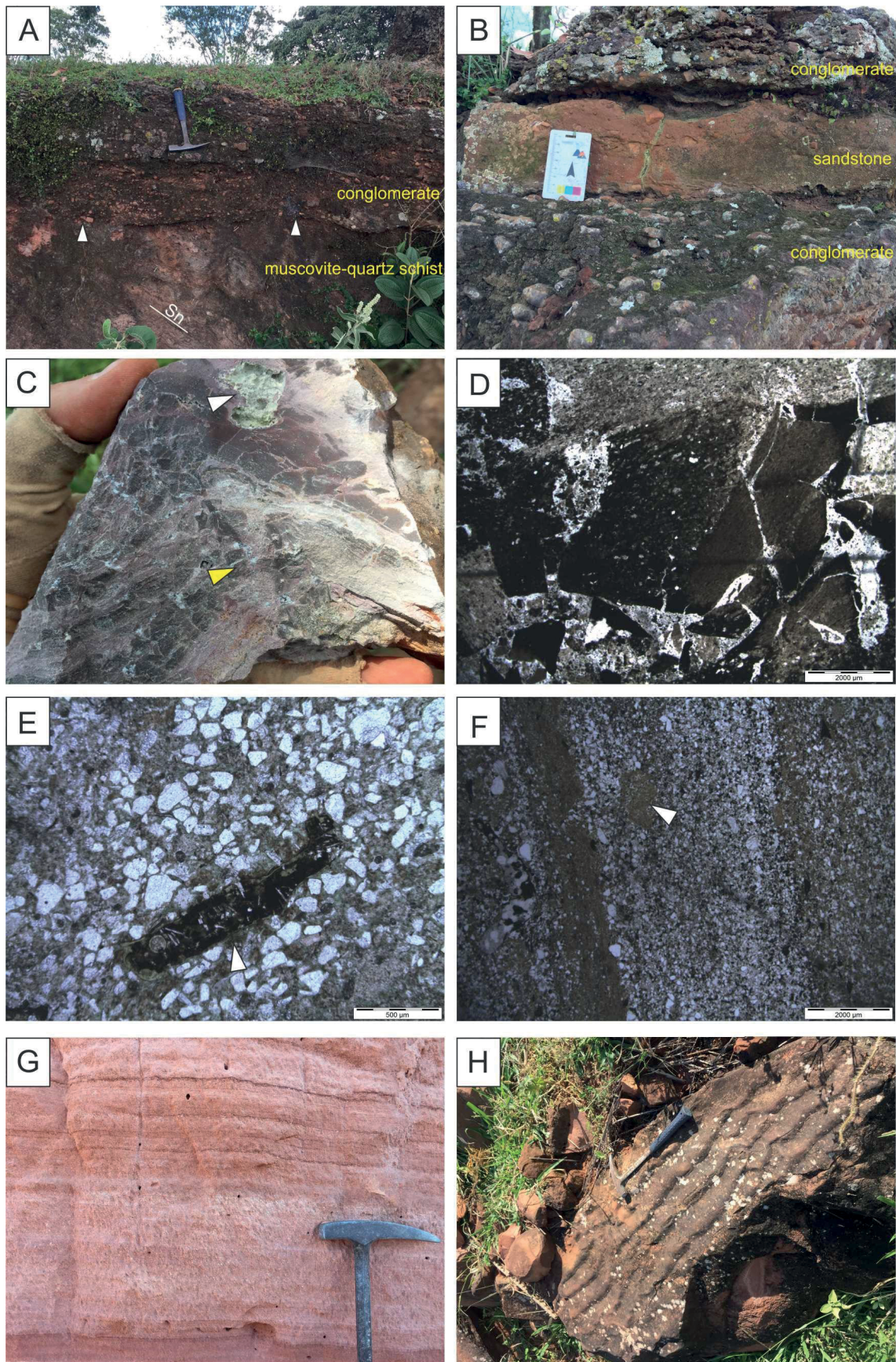


Figure 8. Associated sedimentary deposits: (A) Angular unconformity between Neoproterozoic rocks and alluvial/fluviol sedimentary rocks; the irregular and wavy contact is shown by arrows (FIT44); (B) sandstone sandwiched between two conglomerate layers (FIT44); (C) atectonic fold (yellow arrow) and vug filled with zeolite (white arrow) in very fine sandstone/ siltite (FIT40); (D) deformational breccia with chalcedony-welded fragments in mudstone/siltstone (1.25 parallel polarizer) (FIT40); (E) shard (black) showing plagioclase microlites, vesicle, and celadonite-altered border in a poorly selected matrix-sustained fine sandstone. Here, the well-rounded quartz contribution is poorer than in D; (F) detail of the finer portion of the previous deposit showing lamination in different grain sizes and a fragment extracted from the most clayey portion (white arrow) (FIT38; parallel polarizer); (G) low-angle laminated quartz sandstone rich in plagioclase and opaque minerals (FIT53); (H) asymmetrical wind ripples with local interference (FIT53).

FLOW CORRELATION BASED ON P₂O₅ CONTENT

Attempts to use P₂O₅ content to identify and correlate individual lava flows in LIPs (as in Beane *et al.* 1986, Rosenstengel and Hartmann 2012, Licht 2018, Fernandes *et al.* 2018) resulted in five classes named C36, C43, C52, C62, and C80 (Tab. 3). According to Figures 9 and 10, they are high-Ti magmas called

Pitanga by Peate *et al.* (1992) and represent more primitive terms (MgO > 4.8% = 15 samples) and less primitive terms (MgO < 4.8% = 11 samples). As expected, the incompatible elements P and Ti grow from the most to the least primitive terms.

The data obtained are still insufficient to establish safe correlations and elaborate a chemostratigraphic column, although it is possible to individualize lava flows by this parameter, and some conclusions may be anticipated. When assessing the stratigraphic columns, in which P₂O₅ classes were inserted (Figs. 3A and 3B), an enrichment trend incompatible with the stratigraphic top is found in Logs I and II, while in Log IV, this trend is reversed, with the more primitive terms dominating the stratigraphic top. The most primitive terms predominated in Logs V and VII. Preliminary data indicate that basalt flows from FIT02–FIT12 and FIT01–FIT07 outcrops from Logs I and II may be correlated. Also, in Logs IV, V, and VII, spills FIT35–HL004E–FIT24, FIT37–HLA7, and HLA1–FIT27 seem to be correlated.

Table 3. P₂O₅ basalt classes and their relationship with MgO and TiO₂ mean values.

P ₂ O ₅ classes	samples	P ₂ O ₅ %	MgO %	TiO ₂ %
C36	2	0.356	5.49	3.22
C43	13	0.432	4.84	3.53
C52	3	0.5156	4.21	3.73
C62	7	0.619	3.94	3.82
C80	1	0.806	4.09	3.74

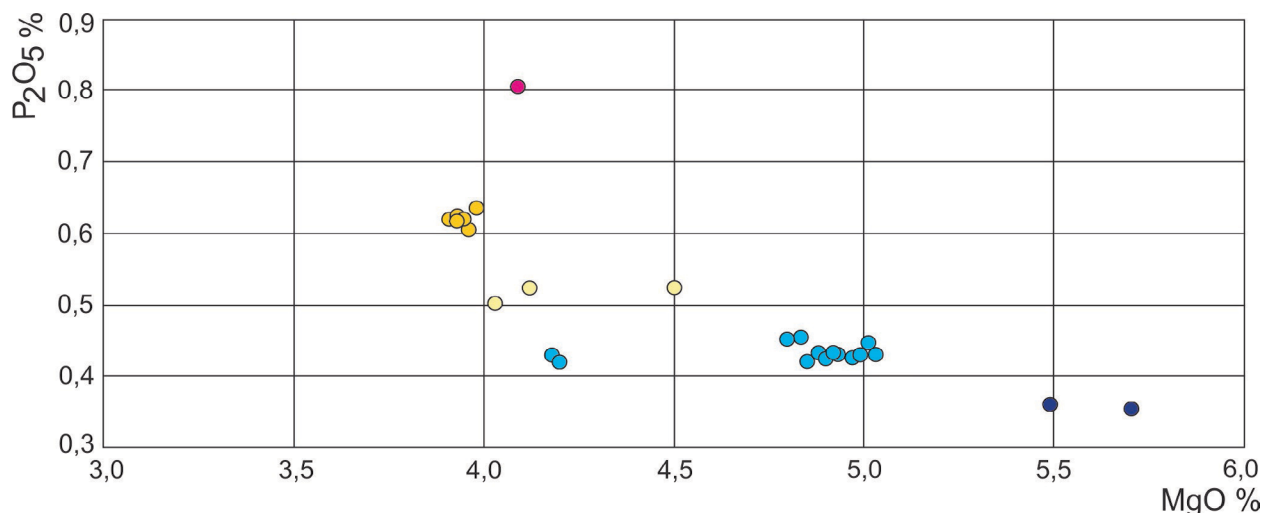


Figure 9. P₂O₅ x MgO diagram. P₂O₅ basalt classes. Deep blue circles = C36; Light blue circles = C43; Yellow circles = C52; Orange circles = C62; Pink circle = C80.

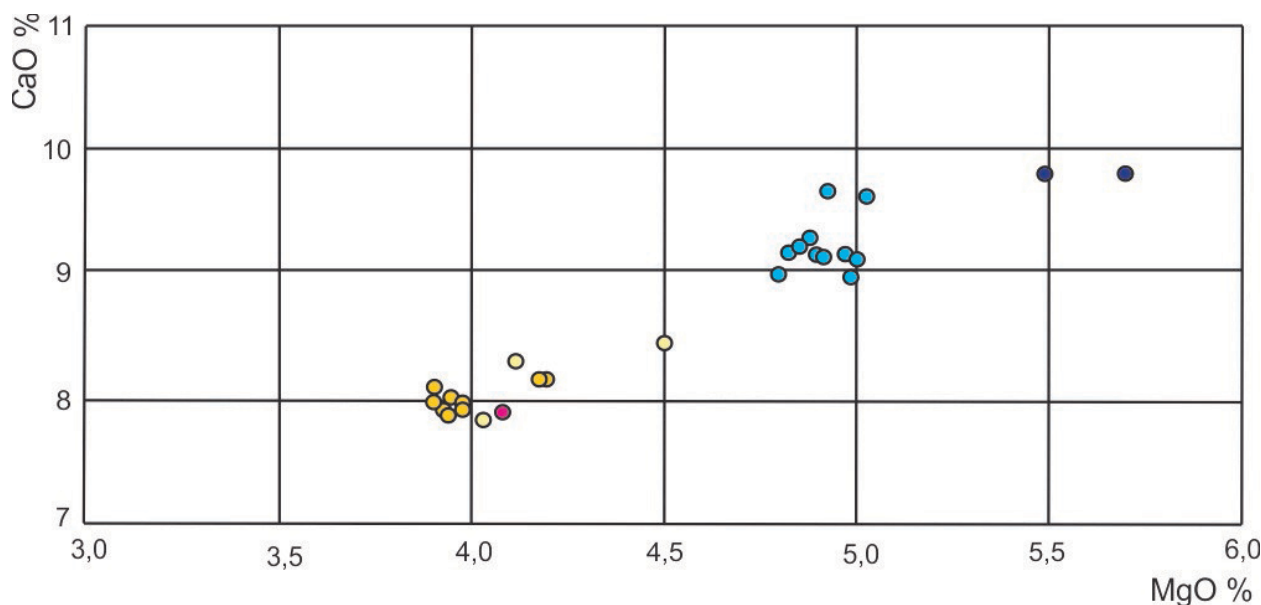


Figure 10. CaO x MgO diagram. P₂O₅ basalt classes correspond to those of Figure 9.

DISCUSSION

Volcanism in the study area was essentially basaltic of tholeiitic character, distributed in lobes, sheets, and rubbly flows, as well as locally pillow lavas and volcanoclastic deposits. These different facies were grouped into compound pahoehoe, simple pahoehoe, rubbly flows, pillow lava, simple pahoehoe/pyroclastic lithofacies associations. Flows may lie over aeolian sands from the Botucatu Formation or the late-Proterozoic lithologies from the Brasília Orogen. They can show relatively thin (up to some meters) intercalations of sedimentary rocks, which can be aeolian, alluvial, lacustrine, or even weathered bole, in the sense of Single and Jerram (2004).

Compound pahoehoe flows are widespread in the center and western portion of the area and occur from the base to near the top of the volcanic sequence (Fig. 3). They are essentially S-type lobes (spongy; Walker 1989). According to Wilmoth and Walker (1993, p. 141), S-type pahoehoe lobes originate when lava emerges from its least-modified tube system due to shorter subsurface residence and less vesicle missing during travel and residence in tubes, as well as surface flows with more than 30% vesicles. In this case, vesicles remain well-distributed in the flow. A lobe is the smallest coherent package of lava, and S-type lobes form with minimal inflation, a consequence of low and intermittent lava flow (Self *et al.* 1998). Discontinuous and thin layers of sediment between lobes reinforce this idea. The size and shape of lobes are variable in this process. Anastomosing architecture is a result of the lobe-by-lobe displacement of lava with minimal loss of heat thanks to the rigid and thin protective crust (Baloga and Glaze 2003).

Not all lobes of the research area are bubble-laden lava. According to Self *et al.* (1998) and references therein, these lobes cannot be called S-type lobes. This scenario brings us to Wilmoth and Walker (1993), who claimed inflated lobes invariably have the basic characteristics of P-type lobes — dense interior and more vesicular exterior —, even when they lack pipe vesicles. However, more data is necessary to call them P-type lobes without pipe vesicles.

Basalt flows, here denominated *simple pahoehoe lithofacies association*, are concentrated in circular areas number II, north of Tupaciguara, and number VI, north of Uberlândia (Fig. 2). We tentatively used this term, but with some reservations since, besides the precariousness of exposures, flow characteristics are not clear enough to differentiate between simple pahoehoe flow and ponded lava, as seen below.

According to Walker (1952), simple pahoehoe flows are products of low effusion rates with sustained lava supply in a paleotopography with declivity lower than 5°. The thin semi-solid carapace that wraps up the lava flow prevents heat loss and allows an inflation process in response to the internal pressure of volatiles. Both Walker (1987) and Philpotts and Lewis (1987) advocate that the core of simple pahoehoe has few cooling joints and may or may not contain horizontal vesicle sheets and vesicle cylinders. Duraiswami *et al.* (2014), based on Aubele *et al.* (1988), Self *et al.* (1998), and their own work, affirm that the upper crust constitutes between 48 and 56% of the total of the flow.

On the other hand, according to Self *et al.* (1998), one way of quickly differentiating ponded flows from inflated flow is by

observing the proportion of the upper crust; the first one varies from < 6% to < 30% (measurements performed on vesicular crust of lava lakes, which are analogous to ponded lava), while inflated flow develops upper vesicular crusts that correspond to 40–60% of the total flow thickness. Rossetti *et al.* (2014) studied deposits from the southern PCMP and defined ponded lava as those flows with tabular geometry, thicknesses up to 50 m, moderately to well-developed columnar fractures, phaneritic texture in the central portion, and vitreous margin.

The presence of tumulus suggests inflation, since this feature develops with a reduction in the surface gradient or an increase in lava influx, according to Walker (1991) (although the first process, in principle, is incompatible with ponded lava). Walker (1991) states that the consequent increase in hydrostatic pressure in a flow bounded by its crust would lead to inflation and, at the same time, to the development of master joints.

Pipe vesicle is a typical feature of simple pahoehoe flows and seen in many CMPs, including the southern part of the PCMP, but not in the study area. According to Wilmoth and Walker (1993), this feature is very common in shallow (< 4°) slopes. In the occurrences studied here, vesicle cylinders are dominantly present in the viscoelastic region and not at the flow core as typical.

The flow exposed in FIT24, which has some distinctive structures of simple pahoehoe flow — tumuli features, holocrystalline texture, and wide lateral continuity —, also has some characteristics of ponded flow, such as upper vesicular crust comprising less than 30% of the exposed flow (probably even smaller), well-developed joints, including colonnade, vesicle cylinders concentrated in the viscoelastic region, and lack of vesicle sheets. FIT07 — another flow tentatively classified as simple pahoehoe flow — was not accessed at top or base and shows marked homogeneity, aphanitic texture, reasonably well-developed columnar fractures, and absence of structures like vesicle sheets and vesicle cylinders. FIT07 also displays features remarkably similar to those presented by Lyle (2000), as a result of water infiltration through master joints that become a secondary cooling surface, accelerating the process and generating hypocrySTALLINE texture. This author also shows recently fallen blocks from that entablature zone (Causeway Tholeiite Member) have clearly broken vertically along the master joints, forming polygons in the horizontal section, delimited by the master joints, which resemble those found in FIT07 (Fig. 5C). These characteristics — which make them difficult to fit into established models — led us to an alternative possibility: a lava flow with low effusion rates that finds a barrier, represented by an irregular paleorelief, can become dammed and stagnant, inflate, and occasionally develop tumuli features, master joints, and, at the same time, vertical joints.

In any case, as noted by Bondre *et al.* (2004a, 2004b), generalizations about lava flow morphologies and emplacement mechanisms across LIPs should be avoided. For example, Self *et al.* (1997) and Sheth (2018) argue that, while the terms compound and simple flows are useful for field work, what seems to be a simple flow in a given outcrop may be a broad flow unit ending against other similar units when followed laterally, making it a compound flow on a larger scale.

Rubbly lava lithofacies association is widespread and seemingly makes up the largest flows in the area, which indicates a relatively high flow rate. Characteristically, they show highly altered flow-top breccia, both by weathering and hydrothermal processes.

According to Bondre and Hart (2008), the described characteristics of flows — less vesicular nuclei and aphanitic texture associated with highly vesicular and venular top breccia — suggest a strong devolatilization during emplacement, with rupture of the rigid crust. Consequently, cooling and viscosity rates increase, limiting crystal growth.

Radial columnar joint structures (like rosettes) were explained by Sheth *et al.* (2017) as related to flow-top breccia detachment. Flow-top breccia fragments are highly vesicular and cold; thus, when they fall into the flow, they “*would not have sunk into the interior owing to their highly vesiculated nature and low densities,*” remaining suspended while inflation and flow advance continued. Their lower temperature would modify the isotherms locally and lead to radial joint columns growing away in a concentric shape around them.

Ring structures related to the Paraná Province have been previously identified in Água Vermelha, Minas Gerais, Brazil (Araújo 1982, Pacheco *et al.* 2018) as structures with ca. 100–200 m of diameter associated with ring dikes. The ring structures identified in Rio Tijuco are smaller, but have great similarity with those in Água Vermelha; although the lava lake was not accessible because of the river water level, and no dikes were found, the same oriented multiple ring structures and conjugate set of fractures (NE and WNW) were present. Additionally, lapilli and tuff deposits were detected, a feature that is apparently less important in Água Vermelha.

We assume that these features originated according to the same model advocated by Pacheco *et al.* (2018), who propose that the basalt flows of the Serra Geral Formation in the Água Vermelha region were extruded through fissures, which evolved to central conduits and lava lakes, when the magma contribution was reduced to the point of sealing much of the fissure, changing it to sparse spots. “*The conduits would present magmatic activity until the cooling of the lava was enough to completely seal the top of the fissures and preserve the circular ring structures*” (p. 146).

According to Self *et al.* (1998), “*long fissures are thermally inefficient and historically have broken down into point sources in a matter of hours to days. Scoria and spatter cones and lava ponds commonly form over these point sources.*”

Sedimentary intercalations have characteristics that suggest climatic differences when compared to the remaining PCMP. Well-rounded quartz grain domain in large cross-stratified deposits refers to aeolian dunes. These deposits can cover the basement (up to 30 m; FIT20, FIT46, FIT51, and FIT58) or be interspersed between lava flows. The same occurs with alluvial deposits (directly over the basement: FIT44, FIT50, FIT53, and FIT42; interspersed between lava flows: FIT26). At the FIT53 point, the initial sedimentation is typically alluvial, changing to aeolian after the first third, and reaching a total of 48 m. At the same time, lacustrine sediments are restricted between lava flows. A single occurrence of weathered bole

(in the sense of Single and Jerram 2004) was identified in FIT24, with thickness between 10 and 40 cm. It is laterally persistent, indicating an interruption in the volcanism, without deposition of another material, under chemical weathering conditions. Also noteworthy is the presence of metamorphic minerals, such as garnet and kyanite, in the fourth interleaving of sedimentary rock in profile 4 (ca. item 4); in the context, it suggests tectonic activity at the Alto Paranaíba Arch, exposing rocks that became the source area for sedimentation.

Figure 3 shows that the distribution of lithofacies associations does not follow a simple pattern. In general, the classic architectural sequence of CMP worldwide is lower compound-braided lava, simple sheet-like pahoehoe, and rubbly flow (Single and Jerram 2004, Duraiswami *et al.* 2014, Rossetti *et al.* 2017). However, in the study area, the compound pahoehoe lithofacies association, for example, is recurrent along the stratigraphic column (Logs I, II, and V).

Also, the complexity of P_2O_5 distribution data, although preliminary and limited, suggests more than one source simultaneously ejecting magma with flow interdigitation and/or multiple supplies of magmatic chamber with volcanism recurrence. We should keep in mind the huge area occupied by the PCMP and the fact that it is largely based on the Paraná Basin. The tectonic compartmentalization of the latter probably influenced the volcanism distribution and morphology (Cañón-Tapia 2018, Licht 2018).

Although they should be assessed and used as reference throughout the PCMP, together, the data attest to the fact that any overgeneralization should be avoided.

CONCLUSIONS

Five lithofacies associations were defined within a polygon bounded by the extreme coordinates 47°32'21"W / 49°16'27"W and 18°23'27"S / 18°58'49"S, in the northern portion of the PCMP in Brazil, namely: compound pahoehoe, simple pahoehoe, rubbly flows, pillow lava and lacustrine sediments, and simple pahoehoe/pyroclastics. Intercalations of sedimentary deposits — varying between 10 cm to 8 m, most of them with less than 2 m — are common and can be typical aeolian, as well as alluvial, lacustrine, or, more rarely, weathered bole. Aeolian sediments are more expressive and predominant in the east and west of the study areas, while those formed in the presence of water dominate the central portion. Basalt flows present clear thickening from east to west, where intercalations of sedimentary deposits become scarce, probably drowned at the bottom. The characteristics shown by the various flows in the study area — broadly dominant entablature structure, hypocrySTALLINE basalts with quench textures, types of associated sedimentary deposits, and pillow lavas — support the idea that water was present during volcanic events. Taking into account the location of the edge of the Alto Paranaíba Arch, which in the Lower Cretaceous was a topographically elevated terrain, the area probably had peridesertic characteristics, where sparse but torrential rains were not unusual. The presence of aeolian sandstone with up to 30 m at the eastern side of the study area reinforces this mixed climatic characteristic.

The complex spatial distribution indicates the need for more detailed studies for a better understanding and precludes the attempt of comparative analysis with the recently established stratigraphy for the southern region of PCMP (Rossetti *et al.* 2017), as well as the P₂O₅-stratigraphy by Fernandes *et al.* (2018) for its north-central region. The recurrence of facies associations in the same stratigraphic section may be related to irregularities in the relief, more than one source of magma acting in the same area simultaneously, instability in the magma

supply, tectonic instability, or more than one of these factors working at the same time.

ACKNOWLEDGMENTS

This work was supported by Fundação de Amparo à Pesquisa do Estado de São Paulo (FAPESP) – Project 2012/06082-6. The original manuscript was greatly improved after comments and suggestions by two anonymous reviewers.

ARTICLE INFORMATION

Manuscript ID: 20200003. Received on: 01/16/2020. Approved on: 05/21/2020.

L.M. wrote the first draft of the manuscript; H.S. prepared and suggested improvements to all figures; V.A. revised and improved the first draft of the manuscript through corrections and suggestions; Author FCN revised the first draft of the manuscript. L.M. and H.S. improved and corrected the manuscript and figures after suggestions by reviewers.

Competing interests: The authors declare no competing interests.

REFERENCES

- Araújo J.S. 1982. *Estruturas Circulares de Água Vermelha*. MS Dissertation, Instituto de Geociências, Universidade de São Paulo, São Paulo, 79 p.
- Aubele J.C., Crumpler L.S., Elston W. 1988. Vesicle zonation and vertical structure of basalt flows. *Journal of Volcanology and Geothermal Research*, **35**(4):349-374. [https://doi.org/10.1016/0377-0273\(88\)90028-5](https://doi.org/10.1016/0377-0273(88)90028-5)
- Baloga S.M., Glaze L.S. 2003. Pahoehoe transport as a correlated random walk. *Journal of Geophysical Research, Solid Earth*, **108**(B1). <http://dx.doi.org/10.1029/2001JB001739>
- Barreto C.J.S., Lima E.F., Scherer C.M., Rossetti L.M.M. 2014. Lithofacies analysis of basic lava flows of the Paraná igneous province in the south hinge of Torres Syncline, Southern Brazil. *Journal of Volcanology and Geothermal Research*, **285**:81-99. <http://dx.doi.org/10.1016/j.jvolgeores.2014.08.008>
- Beane J.E., Turner C.A., Hooper P.R., Subbarao K.V., Walsh J.N. 1986. Stratigraphy, composition and form of the Deccan Basalts, Western Ghats, India. *Bulletin of Volcanology*, **48**(1):61-83.
- Bondre N.R., Duraiswami R.A., Dole G. 2004a. A brief comparison of lava flows from the Deccan Volcanic Province and the Columbia-Oregon Plateau Flood Basalts: Implications for models of flood basalt emplacement. In: Sheth H.C., Pande K. (Eds.). *Magmatism in India through time. Proceedings of the Indian Academy of Sciences (Earth and Planet Sciences)*, **113**:809-817.
- Bondre N.R., Duraiswami R.A., Dole G. 2004b. Morphology and emplacement of flows from the Deccan Volcanic Province, India. *Bulletin of Volcanology*, **66**(1):29-45. <https://doi.org/10.1007/s00445-003-0294-x>
- Bondre N.R., Hart W.K. 2008. Morphological and textural diversity of the Steens Basalt lava flows, Southeastern Oregon, USA: implications for emplacement style and nature of eruptive episodes. *Bulletin of Volcanology*, **70**:999-1019. <https://doi.org/10.1007/s00445-007-0182-x>
- Bryan S.E., Ernst R.E. 2008. Revised definition of Large Igneous Provinces (LIPs). *Earth Science Reviews*, **86**(1-4):175-202. <https://doi.org/10.1016/j.earscirev.2007.08.008>
- Cañon-Tapia E. 2018. The Paraná-Etendeka Continental Flood Province: A historical perspective of current knowledge and future research trends. *Journal of Volcanology and Geothermal Research*, **355**:287-303.
- Chenet A.L., Courtillot V., Fluteau F., Gérard M., Quidelleur X., Khadri S.F.R., Subbarao K.V., Thordarson T. 2009. Determination of rapid Deccan eruptions across the Cretaceous-Tertiary boundary using paleomagnetic secular variation: Constraints from analysis of eight new sections and synthesis for a 3500-m-thick composite section. *Journal of Geophysical Research: Solid Earth*, **114**(B6). <https://doi.org/10.1029/2008JB005644>
- Duraiswami R.A., Gadpallu P., Shaikh T.N., Cardin N. 2014. Pahoehoe-a'a transitions in the lava flow fields of the western Deccan Traps, India: implications for emplacement dynamics, flood basalt architecture and volcanic stratigraphy. *Journal of Asian Earth Sciences*, **84**:146-166. <http://dx.doi.org/10.1016/j.jseaes.2013.08.025>
- Fernandes A.J., Negri F.A., Azevedo Sobrinho J.M., Janasi V.A. 2018. Chemical stratigraphy of the Serra Geral Group in São Paulo. *Brazilian Journal of Geology*, **48**(2):243-261. <https://doi.org/10.1590/2317-4889201720180093>
- Janasi V.A., Freitas V.A., Heaman L.H. 2011. The onset of flood basalt volcanism, Northern Paraná Basin, Brazil: A precise U–Pb baddeleyite/zircon age for a Chapecó-type dacite. *Earth and Planetary Science Letters*, **302**(1-2):147-153. <https://doi.org/10.1016/j.epsl.2010.12.005>
- Jay A.E., Widdowson M. 2008. Stratigraphy, structure and volcanology of the SE Deccan continental flood basalt province: implications for eruptive extent and volumes. *Journal of the Geological Society*, **165**:177-188. <https://doi.org/10.1144/0016-76492006-062>
- Jerram D.A. 2002. Volcanology and Facies architecture of flood basalts. Geological Society of America Special Paper. In: Menzies M.A., Klemperer S.L., Ebinger C.J., Baker J. (Eds.), *Volcanic Rifted Margins*: Geological Society of America Special Paper, **362**:119-132.
- Jerram D.A., Widdowson M. 2005. The anatomy of Continental Flood Basalt Provinces: geological constraints on the processes and products of flood volcanism, *Lithos*, **79**(3-4):385-405. <https://doi.org/10.1016/j.lithos.2004.09.009>
- Licht O.A.B. 2018. A revised chemo-chrono-stratigraphic 4-D model for the extrusive rocks of the Paraná Igneous Province. *Journal of Volcanology and Geothermal Research*, **355**: 32–54. <https://doi.org/10.1016/j.jvolgeores.2016.12.003>
- Lyle P. 2000. The eruption environment multi-tiered columnar basalts lava flows. *Journal of the Geological Society*, **157**:715-722. <https://doi.org/10.1144/jgs.157.4.715>
- McPhie J., Doyle M., Allen R. 1993. *Volcanic Textures*: a guide to the interpretation of textures in volcanic rocks. Hobart: Centre for Ore Deposit and Exploration Studies, University of Tasmania, 1993, 191 p.
- Miall A.D. 1996. *The Geology of Fluvial Deposits. Sedimentary Facies, Basin Analysis and Petroleum Geology*. Berlin, Heidelberg, New York, London, Paris, Tokyo, Hong Kong: Springer-Verlag, 582 p.
- Moraes L.C., Seer H.J. 2018. Pillow lavas and fluvio-lacustrine deposits in the northeast of Paraná Continental Magmatic Province, Brazil, *Journal of Volcanology and Geothermal Research*, **355**:78-86. <http://dx.doi.org/10.1016/j.jvolgeores.2017.03.024>
- Moraes L.C., Seer H.J., Marques L.S. 2018. Geology, geochemistry and petrology of basalts from Paraná Continental Magmatic Province in the Araguaari, Uberlândia, Uberaba and Sacramento regions, Minas Gerais state, Brazil. *Brazilian Journal of Geology*, **48**(2):221-241. <http://dx.doi.org/10.1590/2317-4889201820170091>

- Pacheco F.E.R.C., Caxito F.A., Moraes L.C., Marangoni Y.R., Santos P.R.S., Pedrosa-Soares A.C. 2018. Basaltic ring structures of the Serra Geral Formation at the southern Triângulo Mineiro, Água Vermelha region, Brazil. *Journal of Volcanology and Geothermal Research*, 355:136-148. <http://dx.doi.org/10.1016/j.jvolgeores.2017.06.019>
- Peate D.W., Hawkesworth C.J., Mantovani M.S. 1992. Chemical stratigraphy of the Paraná lavas (South America): classification of magma types and their spatial distribution. *Bulletin of Volcanology*, 55(1-2):119-139. <http://dx.doi.org/10.1007/BF00301125>
- Pedrosa-Soares A.C., Voll E., Profeta A. (Eds.). 2017. *Projeto Triângulo Mineiro e Folha Ouro Preto*. Belo Horizonte: CODEMIG-FUNDEP-UFMG.
- Philpotts A.R., Lewis C.L. 1987. Pipe vesicles – an alternative model for their origin. *Geology*, 15(10):971-974. [https://doi.org/10.1130/0091-7613\(1987\)15%3C971:PVAMFT%3E2.0.CO;2](https://doi.org/10.1130/0091-7613(1987)15%3C971:PVAMFT%3E2.0.CO;2)
- Rosenstengel L.M., Hartmann L.A. 2012. Geochemical stratigraphy of lavas and fault-block structures in the Ametista do Sul geode mining district, Paraná volcanic province, southern Brazil. *Ore Geology Reviews*, 48:332-348. <https://doi.org/10.1016/j.oregeorev.2012.05.003>
- Rossetti L.M., Lima E.F., Waichel B.L., Hole M.J., Simões M.S., Scherer C.M.S. 2017. Lithostratigraphy and volcanology of the Serra Geral Group, Paraná-Etendeka Igneous Province in Southern Brazil: Towards a formal stratigraphical framework. *Journal of Volcanology and Geothermal Research*, 355:98-114. <http://dx.doi.org/10.1016/j.jvolgeores.2017.05.008>
- Rossetti L.M., Lima E.F., Waichel B.L., Scherer C.M., Barreto C.J. 2014. Stratigraphical framework of basaltic lavas in Torres Syncline main valley, southern Parana-Etendeka Volcanic Province. *Journal of South American Earth Sciences*, 56:409-421. <https://doi.org/10.1016/j.jsames.2014.09.025>
- Self S., Keszthelyi L., Thordarson T. 1998. The importance of pahoehoe. *Annual Review of Earth and Planetary Sciences*, 26:81-110. <https://doi.org/10.1146/annurev.earth.26.1.81>
- Self S., Thordarson T., Keszthelyi L.P. 1997. Emplacement of Continental Flood Basalt Lava Flows. In: Mahoney J.J., Coffin M.F. (Eds.). *Large Igneous Provinces: Continental, Oceanic and Planetary Flood Volcanism* American Geophysical Union. Washington: American Geophysical Union, p. 381-410.
- Self S., Widdowson M., Thordarson T., Jay A.E. 2006. Volatile fluxes during flood basalt eruptions and potential effects on the global environment: a Deccan perspective. *Earth and Planetary Science Letters*, 248(1-2):518-532. <https://doi.org/10.1016/j.epsl.2006.05.041>
- Sheth H. 2018. *A Photographic Atlas of Flood Basalt Volcanism*. Berlin: Springer. <https://doi.org/10.1007/978-3-319-67705-7>
- Sheth H., Pal I., Patel V., Samant H., D'Souza J. 2017. Breccia-cored columnar rosettes in a rubbly pahoehoe lava flow, Elephanta Island, Deccan Traps, and a model for their origin. *Geoscience Front*, 8(6):1299-1309. <https://doi.org/10.1016/j.gsf.2016.12.004>
- Single R.T., Jerram D.A. 2004. The 3D facies architecture of flood basalt provinces and their internal heterogeneity: examples from the Palaeogene Skye Lava Field. *Journal of the Geological Society*, 161(6):911-926. <https://doi.org/10.1144/0016-764903-136>
- Valeriano M.M. 2004. *Modelo Digital de Elevação com Dados SRTM disponíveis para América do Sul*. São José dos Campos: INPE / Coordenação de Ensino, Documentação e Programas Especiais (INPE-10550-RPQ/756), 72 p.
- Waichel B.L. 2006. *Estruturação de Derrames e Interações Lava-Sedimento na Porção Central da Província Basáltica Continental do Paraná*. PhD Thesis, Universidade Federal do Rio Grande do Sul, Porto Alegre.
- Waichel B.L., Lima E.F., Viana A.R., Scherer C.M., Bueno G.V., Dutra G. 2012. Stratigraphy and volcanic facies architecture of the Torres Syncline, Southern Brazil, and its role in understanding the Parana-Etendeka Continental Flood Basalt Province. *Journal of Volcanology and Geothermal Research*, 215-216:74-82. <https://doi.org/10.1016/j.jvolgeores.2011.12.004>
- Walker G.P.L. 1952. *Compound and Simple Lava Flows and Flood Basalts*. London: Imperial College London, p. 579-590.
- Walker G.P.L. 1987. Pipe vesicles in Hawaiian basalt lavas: their origin and potential as paleoslope indicators. *Geology*, 15(1):84-87. [https://doi.org/10.1130/0091-7613\(1987\)15%3C84:PVIHBL%3E2.0.CO;2](https://doi.org/10.1130/0091-7613(1987)15%3C84:PVIHBL%3E2.0.CO;2)
- Walker G.P.L. 1989. Spongy pahoehoe in Hawaii: a study of vesicle distribution patterns in basalt and their significance. *Bulletin of Volcanology*, 51:199-209. <https://doi.org/10.1007/BF01067956>
- Walker G.P.L. 1991. Structure, and origin by injection of lava under surface crust, of tumuli, "lava rises", "lava-rise pits", and "lava-inflation clefts" in Hawaii. *Bulletin of Volcanology*, 53(7):546-558. <https://doi.org/10.1007/BF00298155>
- Walker R.G. 1984. General introduction: facies, facies sequences and facies models. In: Walker R.G. (Ed). *Facies Models*. 2ª ed. St. Johns, Geology Association of Canada, p. 1-9.
- Wignall P.B. 2001. Large igneous provinces and mass extinctions. *Earth Science Reviews*, 53(1-2):1-33. [https://doi.org/10.1016/S0012-8252\(00\)00037-4](https://doi.org/10.1016/S0012-8252(00)00037-4)
- Wignall P.B. 2005. The link between Large Igneous Province eruptions and mass extinctions. *Elements*, 1(5):293-297. <https://doi.org/10.2113/gselements.1.5.293>
- Wilmoth R.A., Walker G.P.L. 1993. P-type and S-type pahoehoe: a study of vesicle distribution patterns in Hawaiian lava flows. *Journal of Volcanology and Geothermal Research*, 55(1-2):129-142. [https://doi.org/10.1016/0377-0273\(93\)90094-8](https://doi.org/10.1016/0377-0273(93)90094-8)